



Trade Science Inc.

# Macromolecules

*An Indian Journal**Full Paper*

MMAIJ, 7(1), 2011 [23-30]

## Evolution of the charged structures for small $\text{Si}_n$ clusters

Gui-Ying Wang, Bao-Xing Li\*, Xiao Zhang, Zhi-Wei Ma, Jiao-Jiao Gu, Guo-Bao Li  
 Department of Physics, Microfluidic Chip Institute, and Key Laboratory of Organosilicon Chemistry and Material  
 Technology of Ministry of Education, Hangzhou Normal University, Hangzhou, Zhejiang 310036, (CHINA)

PACS: 36.40.-c; 61.46.-w ; 61.46.Bc

Received: 30<sup>th</sup> October, 2010 ; Accepted: 9<sup>th</sup> November, 2010

### ABSTRACT

We have investigated the evolution of the ground state structures for small  $\text{Si}_n$  ( $n=4-10$ ) clusters as a function of charging by using Full-Potential Linear-Muffin-Tin-Orbital Molecular-Dynamics (FP-LMTO-MD) method. Most of the ionic geometrical configurations from the neutral cluster structures still keep original geometrical configurations except for local structural distortion. The structural distortion is different for different Si clusters with increasing charging. The electrostatic repulsion among the charged atoms and the change of bonding characteristic for some atoms cause the distortion. However, some of the multiply charged structures from the neutral cluster structures are not global minima. We have obtained their ground state structures for  $\text{Si}_n^M$  ( $n=4-10$ ,  $M=0, \pm 1, \pm 2, \pm 3, \pm 4$ ) clusters by the Amsterdam Density Functional (ADF) combined with a single-parent evolution algorithm. © 2011 Trade Science Inc. - INDIA

### KEYWORDS

Silicon cluster;  
 Multiply charged cluster;  
 Molecular-dynamics  
 simulation.

### INTRODUCTION

The electronic and geometric structures for silicon clusters have been extensively studied because of their significant interest and potential application in microelectronics. During the past decades, theoretical and experimental studies are focused on small silicon clusters because larger clusters can fragment into the small clusters. Experimentally, the small silicon clusters with 4, 6, 7 and 10 atoms are much more stable than other clusters<sup>[1-3]</sup>. Most of the theoretical structures for the small neutral silicon clusters have been accepted universally. Except for  $\text{Si}_5$ , the structures of the small  $\text{Si}_n$  ( $n < 8$ ) clusters have been confirmed by anion photoelectron spectroscopy<sup>[4]</sup>, or by Raman<sup>[5]</sup> and infrared<sup>[6]</sup>

measurements on matrix-isolated clusters. We have also investigated the geometrical structures of the small  $\text{Si}_n$  clusters using Full-Potential Linear-Muffin-Tin-Orbital Molecular-Dynamics (FP-LMTO-MD) method<sup>[7-9]</sup>. Our calculated results are in good agreement with experimental values and theoretical results obtained by other methods<sup>[10]</sup>.

Experimentally, more attention has focused on the ionic silicon clusters because of the high ionization energy of the  $\text{Si}_n$  clusters<sup>[2,3,11-18]</sup>. The chemical reactions of the ionic clusters with some small molecules have been studied<sup>[19-21]</sup>. According to a collision-induced dissociation study, the cationic  $\text{Si}_n^+$  clusters containing up to 60 atoms dissociate mainly by loss of  $\text{Si}_6$  or  $\text{Si}_{10}$  species and little by the loss of  $\text{Si}_7$  or  $\text{Si}_{11}$ <sup>[12]</sup>. These are

## Full Paper

consistent with prominent presence of  $\text{Si}_6^+$ ,  $\text{Si}_7^+$ , and  $\text{Si}_{10}^+$  ions in the mass spectra<sup>[3,13]</sup>.

Theoretically, the geometrical structures of the silicon cluster ions have been obtained by employing different dynamics methods<sup>[16-18,22-24]</sup>. It is found that most of the structures for singly charged species are similar to those of their corresponding neutrals, but a few of ionic clusters adopt different geometries as their ground state structures. In addition, some structures are still controversy in the literatures.

Multiply ionized clusters attract scientist's interest because they can fragment into smaller species due to strong coulomb repulsion<sup>[25]</sup>. Study of multiply ionized alkaline clusters in a strong electromagnetic field had been reported<sup>[26]</sup>. For multiply ionized  $\text{Si}_N^M$  ( $N=2-7$ ,  $M=0, \pm 1, \pm 2, \pm 3$ ) clusters, their stability and fragmentations had been investigated by using spin density functional method with the 6-31G\* basis set<sup>[27]</sup>. It was found that the fragmentation of the clusters significantly affects the mass-spectra of the multiply ionized silicon clusters. For doubly ionized silicon cluster cations, large fragmentation energy corresponds to the high peaks at  $N=4$  and  $6$  in mass-spectra. For  $\text{Si}_N^{-2}$  clusters, the peak is predicted to be at  $N=5$ . The theoretical results also suggest that the geometrical structures for the multiply ionized  $\text{Si}_N^M$  clusters are similar to those of their neutrals although some structural distortion occurred. Experimentally, Tsong had obtained mass-spectra for doubly ionized silicon cluster cations<sup>[28]</sup>.

In order to better understand the physical and chemical properties of the  $\text{Si}_n$  clusters and their ions, we have performed careful investigations on the change of geometrical structures for the small  $\text{Si}_n$  ( $n=4-10$ ) clusters as a function of charging using the Full-Potential Linear-Muffin-Tin-Orbital Molecular-Dynamics method. At the same time, global structure optimization has been performed by Amsterdam Density Functional (ADF) combined with a single-parent evolution algorithm. The results are presented in the third section.

## METHOD

The Full-Potential Linear-Muffin-Tin-Orbital Molecular-Dynamics (FP-LMTO-MD) method is a self-consistent implementation of the Kohn-Sham equations in the local-density approximation<sup>[29-32]</sup>. During the mo-

lecular-dynamics calculations, space is divided into two parts: non-overlapping muffin-tin (MT) spheres centered at the nuclei, and the remaining interstitial region. LMTOs are augmented Hankel functions inside the MT spheres, but not in the interstitial region<sup>[32-35]</sup>. Self-consistent field calculations are carried out with a convergence criteria of  $10^{-5}$  a.u. on the total energy and  $10^{-3}$  a.u. on the force.

By using the FP-LMTO-MD method, we have investigated the multiply charged silicon clusters by adding electrons into, or removing electrons from the neutral clusters. In order to search for the ground state structures for the multiply charged clusters, we performed global structure optimization by employing Amsterdam Density Functional (ADF) combined with a single-parent evolution algorithm<sup>[36]</sup>.

In the ADF program<sup>[37]</sup>, molecular orbitals (MOs) were expanded using a large, uncontracted set of Slater-type orbitals: TZ2P<sup>[38]</sup>. The TZ2P basis is an all-electron basis of triple- $\zeta$  quality, augmented by two sets of polarization functions ( $2p$  and  $3d$  on H;  $d$  and  $f$  on heavy atoms). An auxiliary set of  $s$ ,  $p$ ,  $d$ ,  $f$ , and  $g$  STOs was used to fit the molecular density and to represent the Coulomb and exchange potentials accurately in each self-consistent field (SCF) cycle. Geometry optimizations were performed with a generalized gradient approximation (GGA) with Becke Perdew exchange potential.

The methods are suitable for investigating the geometrical and electronic structures of semiconductor and metal clusters<sup>[9,39,40]</sup>. The calculated results from the methods are in good agreement with those obtained by some other advanced molecular dynamics methods<sup>[24]</sup>. In order to compare with those obtained by 6-31G\* and MP4/6-31G\* calculations<sup>[24]</sup> and the experimental values<sup>[41-47]</sup>, our results for small  $\text{Si}_{2-8}$  clusters are presented in TABLE 1. The calculated Si-Si bond lengths are expected to be reliable to within 1-2%. In MP4/6-31G\* calculations, electron correlation effects were included by means of complete fourth order Moller-Plesset perturbation theory with the 6-31G\* basis set (MP4/6-31G\*). This theory has contributions from single, double, triple, and quadruple substitutions from the starting HF determinant and gives reliable binding energies for many calculations. However, comparison with the corresponding experimental values suggests that

about 80–85 % of the true binding energy is obtained. A scale factor of 1.2 empirically corrects for the underestimations, and yields binding energies in good agreement with experiment<sup>[1]</sup>. Using the FP-LMTO-MD method and the ADF program, we have also obtained the same ground state structures for  $\text{Si}_{2-8}$  clusters. The geometrical parameters are in consistent with those obtained by other LDF methods. We haven't listed the values repeatedly here. Although the calculated cohesive energies (binding energy per atom) are larger than the corresponding experimental values, we find that scale factors of 0.77 (for FP-LMTO-MD) and 0.82 (for ADF) empirically correct for the overestimations, and yields binding energies in excellent agreement with experiment values. The use of such a single uniform scale factor does not bias the relative comparisons of the different clusters.

## RESULTS AND DISCUSSIONS

The ground state structure of neutral  $\text{Si}_4$  cluster is a rhombus with symmetry  $D_{2h}$ . Some ionic structures from its neutral are optimized by the FP-LMTO-MD method. The results are shown as figure 1.  $\text{Si}_4^{+4}$ ,  $\text{Si}_4^{+3}$ ,  $\text{Si}_4^{+2}$ ,  $\text{Si}_4^{+1}$ ,  $\text{Si}_4^{-1}$ ,  $\text{Si}_4^{-2}$ ,  $\text{Si}_4^{-3}$ ,  $\text{Si}_4^{-4}$  and  $\text{Si}_4^{-5}$  cluster ions have a similar geometrical structure with the same symmetry (some of ionic structures are not drawn in figure 1). TABLE 2 presents the evolution of bond lengths  $d_{13}$  and  $d_{34}$  as a function of charging. An inspection of the bond lengths showed that both increasing and decreasing charging result in the increase of the bond lengths. In  $\text{Si}_4^{+2}$  and  $\text{Si}_4^{+1}$  cations, the bond length  $d_{13}$  is the shortest among the clusters including its neutral cluster. But the shortest  $d_{34}$  bond length occurs in the  $\text{Si}_4^{-2}$  anion structures. Overall, the neutral structure is more compact than the other ionic structures. In the ionic structures, the charge added or removed will change the bonding characteristics for silicon atoms. Mulliken population analysis shows that charge in the  $\text{Si}_4$  cluster cations trend to distribute into each atom evenly as charge increases. Therefore, if more electrons were removed from  $\text{Si}_4$  cluster, the electronic configuration would transfer from  $2s^22p^2$  into  $2s^22p^1$ . Such electronic configuration easily creates  $sp^2$  hybrid producing ring structure. Cations  $\text{Si}_4^{+4}$  and  $\text{Si}_4^{+3}$  have such ring structures. On the other hand, when one or two electrons

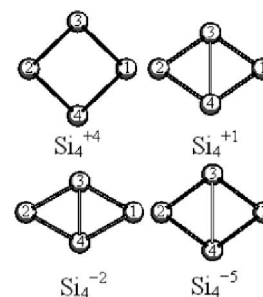


Figure 1 : The ionic structures from neutral  $\text{Si}_4$  cluster

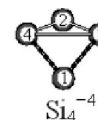


Figure 2 : Global minimum for  $\text{Si}_4^{-4}$  cluster ion

are added into the cluster, most of charge accumulates on atoms 1 and 2. The larger distance between atoms 1 and 2 is resulted from larger electrostatic repulsion between them. However, charge distribution on atoms 3 and 4 trends to increase when more electrons are added into the cluster. Hence, the bond length  $d_{34}$  increases as additional electrons increases.

We have also performed calculations on  $\text{Si}_4^M$  ( $M=\pm 1, \pm 2, \pm 3, \pm 4$ ) cluster ions from neutral  $\text{Si}_4$  cluster by using the ADF program. The results obtained are similar to those in figure 1. But, we cannot obtain the stable structure of  $\text{Si}_4^{+4}$  cation. Furthermore, global optimization based on a single-parent evolution algorithm produces different lowest energy structure of  $\text{Si}_4^{-4}$  anion shown as figure 2.

Figure 3 shows the stable structures of  $\text{Si}_5$  cluster and its ions obtained by the FP-LMTO-MD method. The bond lengths larger than  $3.2\text{\AA}$  are not drawn in figure 2. Neutral  $\text{Si}_5$  cluster has a compact ground state structure. The bond lengths of  $d_{45}$ ,  $d_{12}$  and  $d_{14}$  are  $2.96\text{\AA}$ ,  $3.04\text{\AA}$  and  $2.30\text{\AA}$ , respectively. The ionic structure is not so compact as its neutral structure. Removal of more electrons makes its structure larger in space. Mulliken population analysis suggests that charge on atoms 1 and 3 in positive ion  $\text{Si}_5^{+2}$  are both  $0.52e$ , which is larger than that on other atoms. The weak bond between atoms 1 and 3 is resulted from the electrostatic repulsion between them. After four electrons are taken away, its symmetry becomes  $D_{3h}$  again due to the same charge distribution on three side atoms 1, 2, and 3. Taking away five electrons from  $\text{Si}_5$  cluster makes the structure unstable.

## Full Paper

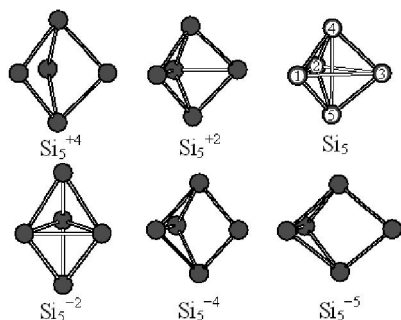


Figure 3 : The structure of neutral  $Si_5$  cluster and the ionic structures obtained from it

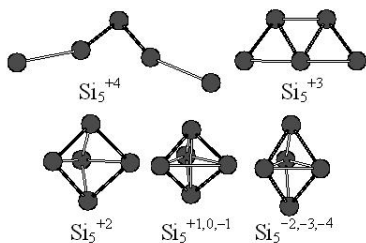


Figure 4 : Global minima for  $Si_5$  cluster and its ions

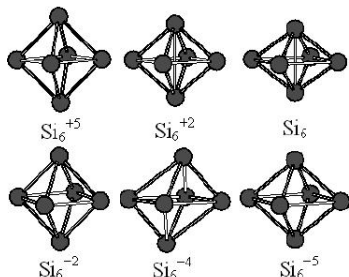


Figure 5 : The structure of neutral  $Si_6$  cluster and the ionic structures obtained from it

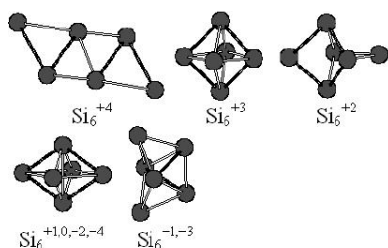


Figure 6 : Global minima for  $Si_6$  cluster and its ions

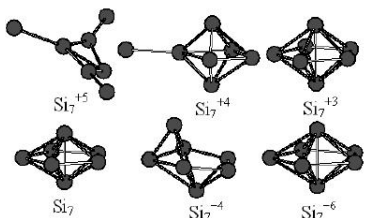


Figure 7 : The structure of neutral  $Si_7$  cluster and the ionic structures obtained from it

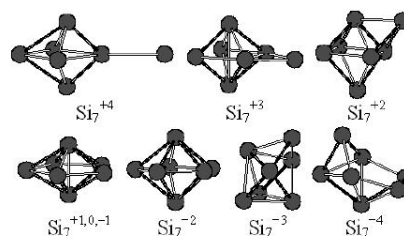


Figure 8 : Global minima for  $Si_7$  cluster and its ions

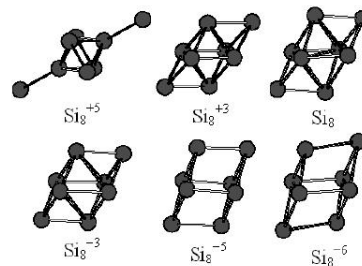


Figure 9 : The structure of neutral  $Si_8$  cluster and the ionic structures obtained from it

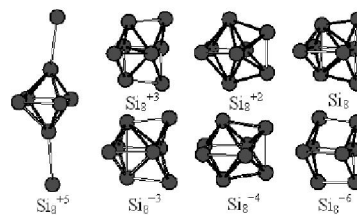


Figure 10 : The structure of neutral  $Si_8$  isomer and the ionic structures obtained from it

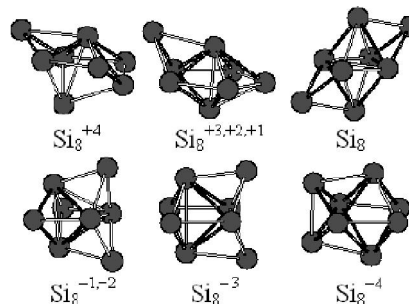


Figure 11 : Global minima for  $Si_8$  cluster and its ions

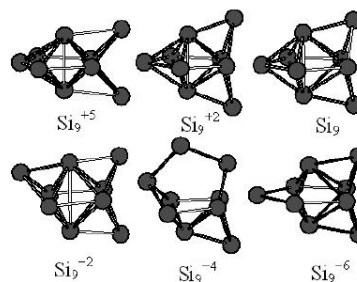


Figure 12 : The structure of neutral  $Si_9$  cluster and the ionic structures obtained from it

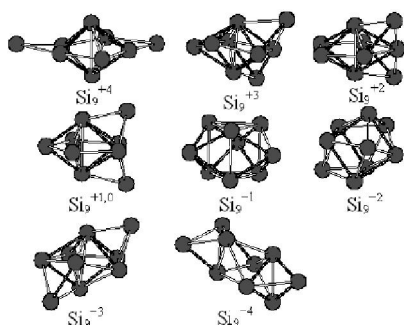


Figure 13 : Global minima for  $\text{Si}_5$  cluster and its ions

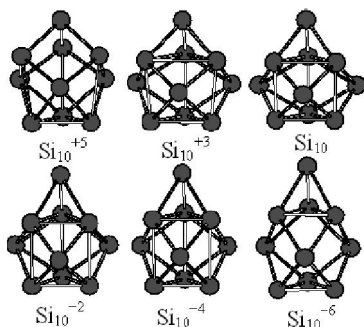


Figure 14 : The structure of neutral  $\text{Si}_{10}$  cluster and the ionic structures obtained from it

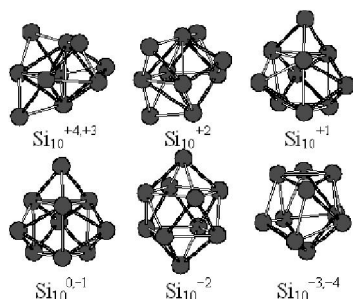


Figure 15 : Global minima for  $\text{Si}_{10}$  cluster and its ions

On the contrary, charge on each apex atom 4, or 5 is  $0.41e$  in the  $\text{Si}_5^{-2}$  ion, whereas charge on each side atoms is  $0.39e$ . As a result, the bond between apex atoms 4 and 5 becomes weak due to larger electrostatic repulsion. Further adding electrons result in more obvious structural distortion. It is found from observing two  $\text{Si}_5^{-4}$  and  $\text{Si}_5^{-5}$  ion structures that the side atom 3 is repulsed due to more charge on it.

ADF global optimization based on a single-parent evolution algorithm produces the ground state structures of neutral and ionic  $\text{Si}_5^M$  ( $M=0, \pm 1, \pm 2, \pm 3, \pm 4$ ) clusters. The results are shown as Fig.4. The structures of  $\text{Si}_5^M$  ( $M=0, \pm 1, \pm 2, -3, -4$ ) clusters are similar to those obtained by the FP-LMTO-MD method although some structures have different symmetry. In particular,

the lowest energy structures for positive  $\text{Si}_5^{+3}$  and  $\text{Si}_5^{+4}$  ions are plane and line-like structures respectively, which differ from those, resulted from neutral  $\text{Si}_5$  cluster.

The neutral and ionic geometrical structures of  $\text{Si}_6$  cluster are shown as figure 5. Experimentally and theoretically,  $\text{Si}_6$  cluster exhibits high stability compared with neighboring clusters. A simple inspection of Fig.5 reveals that charging on  $\text{Si}_6$  cluster does not change its basic geometrical configuration except for local structural distortion. All the positive and negative ion structures are not as compact as its neutral structure. Most severe distortion occurs in  $\text{Si}_6^{-4}$  cluster ions.

By performing structural optimization on the ionic structures from neutral  $\text{Si}_6$  cluster using the ADF program, we can obtain similar structures to the results from the FP-LMTO-MD method. But global search finds that some  $\text{Si}_6$  cluster ions have different ground state structures, shown as Figure 6.  $\text{Si}_6^{+4}$  ion has a plane structure, whereas  $\text{Si}_6^{-}$ ,  $\text{Si}_6^{-3}$  anions have a bicapped tetrahedron. In addition, the structure of  $\text{Si}_6^{+2}$  ion is different from the tetragonal bipyramid of neutral  $\text{Si}_6$  cluster.

For  $\text{Si}_7$  cluster, the situation is somewhat different. After four electrons are taken away, the structure for  $\text{Si}_7^{+4}$  ion can be regarded as an adsorption structure (Figure 7). In this cationic structure, one Si atom seems to be adsorbed on an apex atom of  $\text{Si}_6$  cluster. Removal of one more electron results in planar ionic structure. On the other hand, structural distortion also arises from addition of electrons. It is interesting that there is severe distortion in  $\text{Si}_7^{-4}$  cluster ion. But for  $\text{Si}_7^{-5}$  cluster ion, instead of the increasing distortion, the decreasing distortion is observed. The ADF program produces similar geometrical configurations to the results from the FP-LMTO-MD method. But some of the ground state structures from global optimization are different (Figure 8).

We can obtain two low-lying isomers of  $\text{Si}_8$  cluster by the FP-LMTO-MD method. Its ground state structure is a distorted trans capped octahedron with  $C_2$  (Figure 9). In the previous literatures, the trans capped octahedron with  $C_{2h}$  was the most stable. But, we find that the  $C_{2h}$  can further undergo structural distortion into the  $C_2$ . Another structure is a  $C_{2v}$  bicapped octahedron (Figure 10) obtained by capping the adjacent faces. The latter lies  $0.39$  eV above the former. When five electrons are removed from its ground state structure, two atoms become adatom, which is somewhat

## Full Paper

**TABLE 1 :** Calculated total binding energy ( $E_t$ , in eV), cohesive energy ( $E_c$ , in eV), scaled cohesive energy ( $E_s$ , in eV), and the measured cohesive energy ( $E_{\text{exp}}$ , in eV) by Knudsen mass spectrometers. The HF/6-31G\* and MP4/6-31G\* calculations are cited from Ref.<sup>[24]</sup>. The experimental results are quoted from Ref.<sup>[41-47]</sup>

Cluster	Si <sub>2</sub>	Si <sub>3</sub>	Si <sub>4</sub>	Si <sub>5</sub>	Si <sub>6</sub>	Si <sub>7</sub>	Si <sub>8</sub>
$E_t$ (HF/6-31G*)	1.47	2.96	5.90	7.24	9.90	12.08	13.20
$E_t$ (MP4/6-31G*)	2.60	6.34	10.57	13.74	18.02	22.16	24.31
$E_t$ (FP-LMTO-MD)	4.05	9.97	15.81	21.30	26.97	32.61	36.34
$E_t$ (ADF)	4.32	9.42	15.13	19.96	24.99	29.98	33.68
$E_c$ (HF/6-31G*)	1.30	2.11	2.64	2.75	3.00	3.17	3.04
$E_c$ (FP-LMTO-MD)	2.02	3.32	3.95	4.26	4.50	4.66	4.54
$E_c$ (ADF)	2.16	3.14	3.78	3.99	4.17	4.28	4.21
$E_s$ (MP4/6-31G*)	1.56	2.54	3.17	3.30	3.60	3.80	3.65
$E_s$ (FP-LMTO-MD)	1.56	2.54	3.05	3.28	3.47	3.59	3.50
$E_s$ (ADF)	1.77	2.57	3.10	3.27	3.42	3.51	3.45
$E_{\text{exp}}$	1.66	2.44	2.99	3.24	3.43	3.53	3.54

similar to  $\text{Si}_7^{+4}$  cluster ion. The negative  $\text{Si}_8$  cluster structures still remain similar geometrical configuration to its neutral cluster (Figure 9). For the  $\text{C}_{2v}$  structure, the similar situation is observed. It is interesting that the geometry of  $\text{Si}_8^{+2}$  cation looks like that of  $\text{Si}_8^{-4}$  anion (Figure 10). The ADF program can obtain similar results. But, if global structure optimization is performed, some different lowest energy structures are obtained. The results are presented in figure 11.

Figure 12 presents the stable structures of  $\text{Si}_9$  cluster and its ions obtained by the FP-LMTO-MD method. According to figure 12, the positive ions still keep the bicapped pentagonal bipyramid structure. But the negative ions undergo significant structural distortion. Among the structures, the distortion in  $\text{Si}_9^{-4}$  ion is the most severe. If the ADF program optimizes all the ionic structures from neutral  $\text{Si}_9$  cluster, similar results are obtained but their structural distortion is not as severe as that in the FP-LMTO-MD method. However, global optimization present some new structures for  $\text{Si}_9$  cluster ions, shown as figure 13.

$\text{Si}_{10}$  cluster is also an important because of its high stability like  $\text{Si}_4$  and  $\text{Si}_6$  clusters. Figure 14 shows its neutral and ionic structures. Similar to  $\text{Si}_4$  and  $\text{Si}_6$  clusters, the cationic and anionic structures of  $\text{Si}_{10}$  cluster keep its neutral geometrical configuration basically even though local distortion exists. Single-parent evolution algorithm shows the results in figure 15. Except for neu-

tral  $\text{Si}_{10}$  cluster and its singly charged ions, other ionic structures are different from each other.

According to the discussions above, if the ionic structures from neutral clusters are optimized, some local structural distortion occurs. But most of them still keep original geometrical configurations. The results are in agreement with those obtained by Hashimoto et. al.. Our calculated results show that the influence of charge on the structures from neutral clusters with 4, 6 and 10 atoms is less compared with the other clusters, suggesting the clusters are more stable. But global structure optimization suggests that some charged clusters adopt different geometrical configurations from the neutral clusters. Our calculated results for neutral and singly charged  $\text{Si}_n$  ( $n=4-10$ ) clusters are in good agreement with those computed by other methods<sup>[15,17,18,22,23]</sup>. The structure of  $\text{Si}_6^-$  differs from that of the neutral  $\text{D}_{4h}$  tetragonal bipyramid. The ground states for  $\text{Si}_8^+$ ,  $\text{Si}_8^0$ , and  $\text{Si}_8^-$  are entirely dissimilar:  $\text{C}_s$  capped pentagonal bipyramid,  $\text{C}_2$  distorted bicapped octahedron, and  $\text{C}_{2v}$  tetracapped tetrahedron, respectively. The ground state for  $\text{Si}_9^-$  is a tricapped trigonal prism but that for  $\text{Si}_9^0$  and  $\text{Si}_9^+$  is bicapped pentagonal bipyramid.

The electronic configuration of silicon atom is  $3s^23p^2$ . It usually adopt  $sp^3$  hybrid. Therefore, Si atom hardly forms single or double bonds with other Si atoms in the clusters. Sometimes, even if there are the structures with single or double bonds, they are usually not very stable. When the electrons are removed from Si atom, its electronic configuration changes. The p electron in  $3s^23p^1$  configuration forms single  $\sigma$  bond with neighbor atoms easily. The bonding characteristics in  $\text{Si}_7^{+4}$ ,  $\text{Si}_7^{+5}$  and  $\text{Si}_8^{+5}$  ions probably belong to the situation. In addition, configuration  $3s^23p^1$  can also produce edge atom with double bonds or planar structures by  $sp^1$  or  $sp^2$  hybrid.  $\text{Si}_5^{+4}$  and  $\text{Si}_7^{+5}$  ion structures probably arise from the bonding characteristics. On the other hand, the electrostatic repulsion between the positive atoms is another reason creating structural distortion. When the electrons are added into the clusters, new  $\pi$  bonds probably form between the atoms with additional electrons, which cause the increase of some bond strength. Of course, the negative atoms would be repulsed because of the electrostatic repulsion. The equilibrium bond lengths depend on the strength of the two forces.

**TABLE 2 : Change of bond lengths  $d_{13}$  and  $d_{34}$  (in Å) for  $\text{Si}_4$  cluster and its ions as a function of charging**

Bond	Structure									
	$\text{Si}_4^{+4}$	$\text{Si}_4^{+3}$	$\text{Si}_4^{+2}$	$\text{Si}_4^{+1}$	$\text{Si}_4$	$\text{Si}_4^{-1}$	$\text{Si}_4^{-2}$	$\text{Si}_4^{-3}$	$\text{Si}_4^{-4}$	$\text{Si}_4^{-5}$
$d_{13}$	2.96	2.46	2.29	2.29	2.31	2.31	2.33	2.37	2.49	2.65
$d_{34}$	4.11	3.45	3.21	2.66	2.39	2.33	2.28	2.45	2.73	3.16

**TABLE 3 : Adiabatic ionization potentials IP(I), IP(II), IP(III), and IP(IV) (in eV) are the amount of energy needed when the cluster loses one, two, three and four electrons from its neutral state respectively, whereas adiabatic electron affinities EA(I), EA(II), EA(III) and EA(IV) (in eV) are the amount of energy released when the cluster obtains one, two, three and four electrons referring to its neutral state respectively**

IP, EA	Cluster							
	$\text{Si}_4$	$\text{Si}_5$	$\text{Si}_6$	$\text{Si}_7$	$\text{Si}_8$	$\text{Si}_9$	$\text{Si}_{10}$	
IP(I)	8.03	8.36	7.94	8.17	7.32	7.56	8.01	
IP(II)	20.72	21.69	20.44	20.31	18.60	19.09	20.32	
IP(III)	39.96	39.56	37.65	36.42	34.78	34.92	35.20	
IP(IV)	/	62.60	59.60	57.19	54.81	53.84	53.75	
EA(I)	2.00	2.21	1.89	1.79	2.12	1.81	2.23	
EA(II)	-0.52	0.82	0.41	0.06	0.91	0.22	1.27	
EA(III)	-7.72	-6.38	-6.55	-6.34	-4.73	-5.18	-3.98	
EA(IV)	-18.02	-16.25	-16.54	-15.52	-12.85	-13.46	-12.25	

TABLE 3 presents adiabatic ionization potentials IP(I), IP(II), IP(III), IP(IV) and adiabatic electron affinities EA(I), EA(II), EA(III) and EA(IV) of  $\text{Si}_n$  ( $n=4-10$ ) clusters. The results are obtained by using the ADF program with a generalized gradient approximation (GGA) combined with Becke Perdew exchange potential. IP(I), IP(II), IP(III), and IP(IV) are the amount of energy needed when one, two, three and four electrons are lost from its neutral state, respectively. Whereas EA(I), EA(II), EA(III) and EA(IV) are the amount of energy released when the neutral state obtains one, two, three and four electrons, respectively. It is found from observing TABLE 3 that both of the adiabatic ionization potentials and the adiabatic electron affinities trend to decrease overall as the atom number increases. In addition, all of the EA(I)s are positive, suggesting that the clusters have a tendency to gain an electron under normal conditions, as it is energetically favorable to do so. But, the EA(II)s in TABLE 3 are also positive except for  $\text{Si}_4$ . The values are small universally, but  $\text{Si}_{10}$  cluster has larger EA(II) relatively to its neighboring clusters. All of the negative EA(III)s and EA(IV)s show

that the silicon clusters gain three or more electrons under normal conditions difficultly.

## CONCLUSIONS

On charging the ground state structures and their isomers of the small neutral  $\text{Si}_n$  ( $n=4-10$ ) clusters, they undergo structural distortion to some extent. The distortion depends on charge and their structures. The structural distortion of the charged  $\text{Si}_4$ ,  $\text{Si}_6$  and  $\text{Si}_{10}$  clusters is smaller relatively to other clusters, suggesting the clusters are more stable than their neighboring. The structural distortion results from the electrostatic repulsion among the charged atoms and the change of bonding characteristic. In addition, removal of charge causes the clusters to be unstable easily. The adiabatic ionization potentials and adiabatic electron affinities trend to decrease overall as the clusters become large. It is energetically favorable for the silicon clusters gain an electron from its neutral state. Most of the clusters still can release energy after they gain two electrons. But, they obtain three electrons or more difficultly. Global structure optimization shows that some of the ionic structures from neutral clusters are not the most stable. Some multiply charged clusters adopt other structures as their ground state structures.

## ACKNOWLEDGEMENTS

A Foundation for the Author of National Excellent Doctoral Dissertation of PR China (Grant No. 200320), the Natural Science Foundation of Zhejiang Province (Grant No. Y6100098) and Natural Nature Science Foundation of china (Grant No. 10674039) supported this work.

## REFERENCES

- [1] K.Raghavachari; Phase Transit, **61**, 24-26 (1990).
- [2] Q.L.Zhang, Y.Liu, R.F.Curl, F. K.Tittel, R.E.Smalley; J.Chem.Phys., **88**, 1670 (1988).
- [3] S.Wei, R.N.Barnett, U.Landman; Phys.Rev.B, **55**, 7935 (1997).
- [4] C.C.Arnold, D.M.Neumark; J.Chem.Phys., **99**, 3353 (1993).
- [5] E.C.Honea; Nature, **366**, 42 (1993).

**Full Paper**

- [6] S.Li, R.J.Van Zee, W.Weltner Jr., K.Raghavachari; Chem.Phys.Lett., **243**, 275 (1995).
- [7] B.X.Li, P.L.Cao; Phys.Rev.B, **62**, 15788 (2000).
- [8] B.X.Li, P.L.Cao, M.Jiang; Phys.Stat.Sol.B, **218**, 399 (2000).
- [9] B.X.Li, P.L.Cao, S.C.Zhan; Phys.Lett.A, **316**, 252 (2003).
- [10] Vasiliev, S.Ogut, J.R.Chelikowsky; Phys.Rev.Lett., **78**, 4805 (1997).
- [11] K.Fuke, K.Tsukamoto, F.Misaizu, M.Sanekata; J.Chem.Phys., **99**, 7807 (1993).
- [12] M.F.Jarrold, E.C.Honea; J.Phys.Chem., **95**, 9181 (1991).
- [13] S.M.Beck, J.M.Andrews; J.Chem.Phys., **91**, 4420 (1989).
- [14] R.R.Hudgins, M.Lmai, M.F.Jarrold, P.Dugourd; J.Chem.Phys., **111**, 7865 (1999).
- [15] N.Binggeli, J.R.Chelikowsky; Phys.Rev.Lett., **75**, 493 (1995).
- [16] A.A.Shvartsburga, B.Liu, M.F.Jarrold, K.M.Ho; J.Chem.Phys., **112**, 4517 (2000).
- [17] J.Muller, B.Liu, A.A.Shvartsburga, S.Ogut, J.R.Chelikowsky, K.W.M.Siu, K.M.Ho, G.Gantefor; Phys.Rev.Lett., **85**, 1666 (2000).
- [18] B.Liu, Z.Y.Lu, B.Pan, C.Z.Wang, K.M.Ho; J.Chem.Phys., **109**, 9401 (1998).
- [19] M.F.Jarrold, J.E.Bower, K.Creegan; J.Chem.Phys., **90**, 3615 (1989).
- [20] W.R.Creasy, A.O'Keefe, J.R.McDonald; J.Phys.Chem., **91**, 2848 (1987).
- [21] U.Ray, M.F.Jarrold; J.Chem.Phys., **94**, 2631 (1991).
- [22] J.R.Chelikowsky, J.C.Phillips; Phys.Rev.Lett., **63**, 1653 (1989).
- [23] K.Raghavachari, C.M.Rohlfing; J.Phys.Chem., **94**, 3670 (1991).
- [24] K.Raghavachari, C.M.Rohlfing; J.Chem.Phys., **89**, 2219 (1988).
- [25] O.Echt, T.D.Mark; Ser.Chem.Phys., Edited by H.Haberland; Berlin, Heidelberg, New York, Tokyo, Hong Kong, Barcelona, Budapest, Springer-Verlag, Berlin, **56**, 183 (1994).
- [26] M.B.Smirnov, V.P.Krainov; J.Exp.& Theor.Phys., **88**, 1102 (1999).
- [27] K.Hashimoto, M.Okamoto, K.Takayanagi; Eur.Phys.J.D, **2**, 75 (1998).
- [28] T.T.Tsong; Appl.J.Vac.Sci.Technol.B, **6**, 1425 (1985).
- [29] M.Methfessel, M.V.Schilfgaard; Int.J.Mod.Phys.B, **7**, 262 (1993).
- [30] M.Methfessel, M.V.Schilfgaard; Phys.Rev.B, **48**, 4937 (1993).
- [31] M.Methfessel; Phys.Rev.B, **38**, 1537 (1988).
- [32] M.Methfessel, C.O.Rodriguez, O.K.Anderson; Phys.Rev.B, **40**, 2009 (1989).
- [33] W.Kohn, L.J.Sham; Phys.Rev., **140**, A1133 (1965).
- [34] O.K.Andersen; Phys.Rev.B, **12**, 3060 (1975).
- [35] M.Springborg, O.K.Andersen; J.Chem.Phys., **87**, 7125 (1987).
- [36] I.Rata, A.A.Shvartsburg, M.Horoi, T.Frauenheim, K.W.M.Siu, K.A.Jackson; Phys.Rev.Lett., **85**, 546 (2000).
- [37] ADF2007.01; SCM, Theoretical Chemistry, Vrije Universiteit: Amsterdam, The Netherlands, (2007).
- [38] E.van Lenthe, E.J.Baerends; J.Comput.Chem., **24**, 1142 (2003).
- [39] B.X.Li; Phys.Rev.B, **71**, 235311 (2005).
- [40] C.H.Yao, B.Song, P.L.Cao; Phys.Rev.B, **70**, 195431 (2004).
- [41] T.Bachels, R.Schafer; Chem.Phys.Lett., **324**, 365 (2000).
- [42] R.W.Schmude, Q.Ran, K.A.Gingerich, J.E.Kingcade; J.Chem.Phys., **102**, 2574 (1995).
- [43] R.W.Schmude, Q.Ran, K.A.Gingerich; J.Chem.Phys., **99**, 7998 (1993).
- [44] Q.Ran, R.W.Schmude, M.Miller, K.A.Gingerich; Chem.Phys.Lett., **230**, 337 (1994).
- [45] K.A.Gingerich, Q.Ran, R.W.Schmude; Chem.Phys.Lett., **256**, 274 (1996).
- [46] J.C.Grosman, L.Mitas; Phys.Rev.Lett., **74**, 1323 (1995).
- [47] G.Meloni, K.A.Gingerich; J.Chem.Phys., **115**, 5470 (2001).